ELSEVIER

Materials Science and Engineering C 19 (2002) 255–262

MATERIALS SCIENCE & ENGINEERING C

www.elsevier.com/locate/msec

Layer-by-layer self-assembly strategy for template synthesis of nanoscale devices

N.I. Kovtyukhova [a,b,*], B.R. Martin [a], J.K.N. Mbindyo [a], T.E. Mallouk [a,1], M. Cabassi [c], T.S. Mayer [c]

[a] *Department of Chemistry, Pennsylvania State University, University Park, PA 16802, USA*
[b] *Institute of Surface Chemistry, N.A.S.U., 17, General Naumov Str., 03680 Kyiv, Ukraine*
[c] *Department of Electrical Engineering, Pennsylvania State University, University Park, PA 16802, USA*

Abstract

A combined membrane replication/layer-by-layer synthetic approach to preparing nanoscale rod-shaped rectifiers is described. Alumina and polycarbonate (PC) membranes (pore diameters 200, 100 and 70 nm) were used as templates for the electrochemical preparation of free-standing Au nanowires several microns in length. Wet layer-by-layer self-assembly of nanoparticle (TiO_2 or ZnO)/polymer multilayer films was performed inside the membrane pores in two ways. (1) Growing the film between metal electrodeposition steps to give in-wire junctions; (2) first coating the membrane walls with multilayer films, and then growing nanowires inside the resulting tubules to give concentric structures. TiO_2/PSS, ZnO/PSS (PSS = polystyrenesulfonate) and ZnO/PAN (PAN = polyaniline) assembly was driven by electrostatic and covalent-coordination interactions, respectively. The current–voltage (I–V) characteristics of nanowires containing semiconductor nanoparticles show current rectifying behavior. Current rectification appears to arise at the oxide semiconductor–metal interface. Switching behavior and hysteresis, which was found in all devices, was particularly evident in junctions containing anionic PSS and cationic TiO_2 particles, and less evident in ZnO-containing devices.

Keywords: Layer-by-layer self-assembly; Nanoscale devices; Rectification

1. Introduction

Current miniaturization trends in electronics and electromechanical systems have stimulated the development of radically new concepts for fabricating electronic nanostructures. One prospective approach to this problem is to integrate conventional lithographic structures with chemically synthesized nanoscale components. The latter include molecule- and polymer-based devices that can function as rectifiers, transistors and switches [1–8]. A real challenge in the practical use of these devices is the problem of making the appropriate connections between nanoscale devices, and their integration into the larger scale circuits. Towards this end, some functional circuits based on molecular diodes [9], and nanoscale crossbar arrays that contain bistable memory elements [10–12], have recently been proposed. In these crossbar arrays, a "bit" at each crossing point between long wires is set to a high or low conductance state. Switching of this bit between states, which corresponds to changing between logical 0 and 1, is done electrically and therefore requires a device with hysteresis in its current–voltage (I–V) characteristics. In addition, current rectification is needed at each crossing point to prevent cross-talk between bits in the same array.

Using methods originally developed by Al-Mawlawi et al. [13], Nishizava et al. [14], Menon and Martin [15], Martin [16], Wang et al. [17], Martin and Parthasarathy [18], and Lakshmi et al. [19], we have synthesized nanowires by electrochemical replication of alumina and polycarbonate (PC) membranes [20–22]. The advantage of this technique over other solution-phase and vapor-phase methods for making metallic nanowires is that it permits the introduction of "stripes" along the length of the wires by sequentially plating one metal after another. Different metals have different surface chemistry, and this allows one to tether specific molecules to different stripes. For example, it is possible to use interactions between single-

* Corresponding author. Department of Chemistry, Pennsylvania State University, 152 Davey Lab, University Park, PA 16802, USA.
E-mail address: nina@chem.psu.edu (N.I. Kovtyukhova).
[1] Also corresponding author.

0928-4931/02/$ - see front matter
PII: S0928-4931(01)00395-2

stranded DNA [22] on the stripes to program the adhesion of nanowires to each other.

Wet layer-by-layer self-assembly is a chemical method for making functional thin film structures from polymers and nanoparticles [23,24]. This method involves the sequential adsorption of inorganic colloidal particles and/or organic macromolecules as monolayers, allowing one to control the sequence of deposition of components with nanometer precision [25–31]. Several kinds of interesting electronic devices have now been synthesized using this technique [30–36], including rectifying diodes [29–32] and electroluminescent devices [35].

Combining advantages of both template replication and layer-by-layer assembly techniques allows preparing nanowires that contain concentric polymer and nanoparticle/polymer structures or in-wire junctions [37,38]. Recently, we showed that by using oxide semiconductor nanoparticles (ZnO or TiO_2) as the cationic component of the layer-by-layer assembly, one can make nanowires that have in-wire or crosspoint rectifying junctions [38]. While current rectification effects were expected in these devices from previous experience with planar semiconductor–polyelectrolyte structures [29–32], an unexpected hysteresis or switching effect was also observed [38]. In this

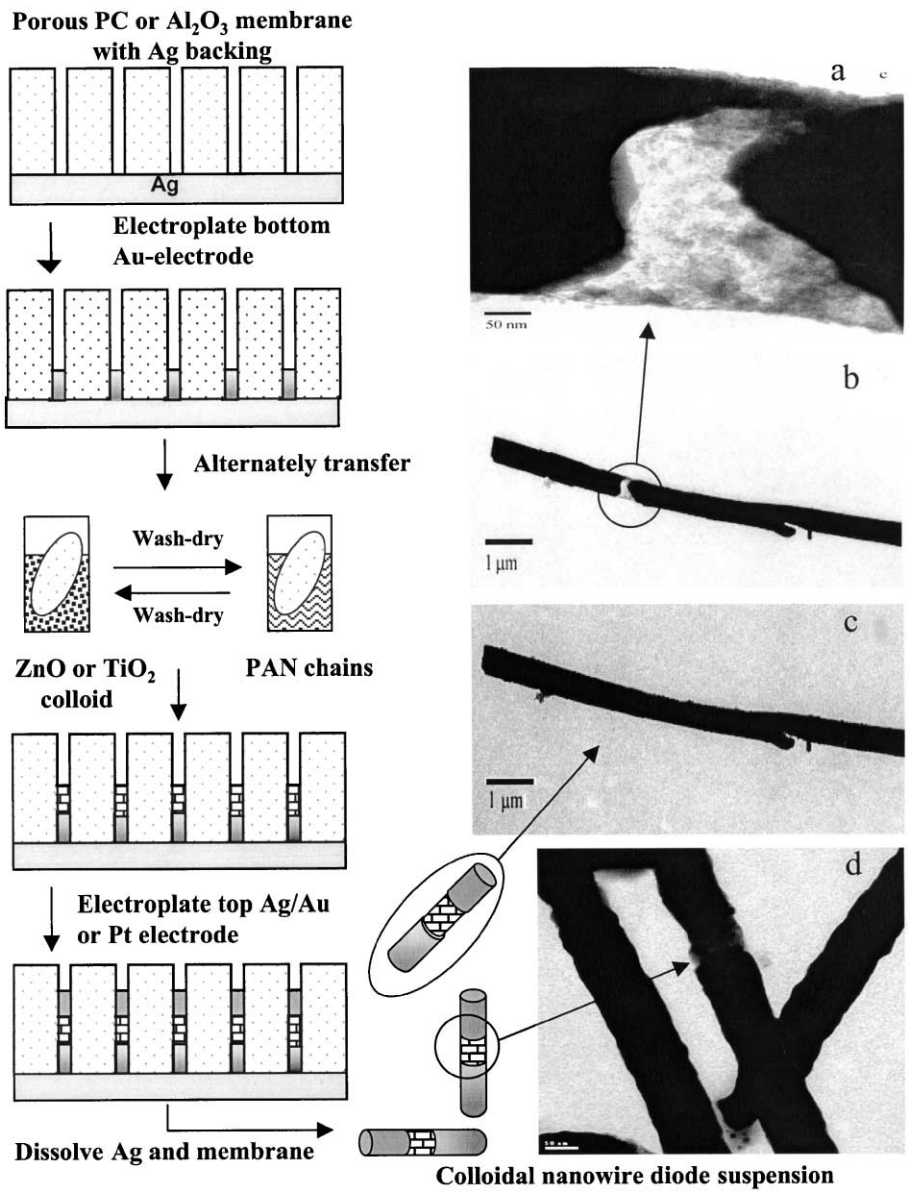

Fig. 1. (Left) Scheme for the preparation of in-wire semiconductor thin-film devices. (Right) (a–c) High- and low-resolution TEM images of the 4 C Au/$(TiO_2/PAN)_{10}$/2 C Ag/4 C Au device prepared using the alumina membrane treated with ethyltriethoxy silane: (a,b) nanoparticle junction (end of the bottom Au electrode on the right). These TEM images were taken after focusing the electron beam for several seconds; (c) the image taken immediately after focusing the electron beam; (d) TEM image of an Au/Ag/$(ZnO/PAN)_9TiO_2$/Au nanowires prepared in a PC membrane. Nanoparticle junction is seen between the two metals.

paper, we examine this effect in more detail. In particular, we explore the effect of in-wire and crosspoint polymer–metal junctions with both cationic and anionic polyelectrolytes, which charge compensate anionic or cationic semiconductor particles deposited at high or low pH, respectively.

2. Experimental details

Two hundred-nanometer pore diameter Whatman Anopore disks (Al_2O_3 membranes) and OSMONICS Poretics, PC membranes were used as templates for nanowire synthesis. TiO_2 and ZnO colloids were prepared as described elsewhere [30,31]. Aqueous (20 wt.%) poly(sodium 4-styrenesulfonate) (PSS), was purchased from Aldrich. The emeraldine base (EB) form of polyaniline (PAN) was prepared as described by Chiang and MacDiarmid [39] and was used as a 0.015 wt.% solution in dimethyl formamide.

2.1. Device structures in which the semiconductor/polymer films are sandwiched between two segments of a nanowire

These devices were synthesized according to the scheme shown in Fig. 1. This process involves four steps: electro-

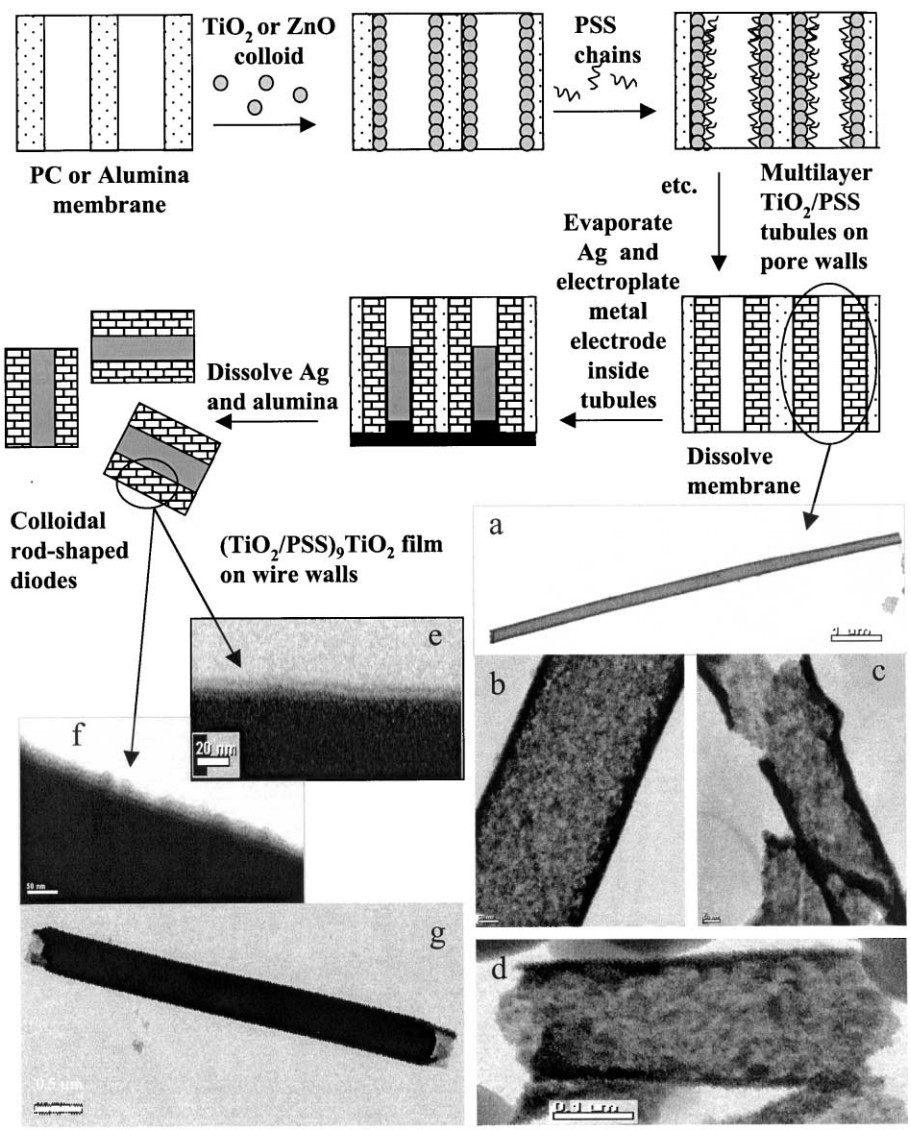

Fig. 2. (Top) Scheme for the synthesis of concentric Au/(semiconductor/polymer) structures by layer-by-layer assembly of multilayer TiO_2(ZnO)/PSS tubules on the pore walls followed by electrochemical or electroless plating of metal rods inside the tubules. (Bottom) TEM images of (a–c) $(TiO_2/PSS)_5TiO_2$ tubules prepared in 200-nm-diameter pores of alumina (a,b) and PC (c) membrane; (d) (ZnO/PSS)ZnO tubules prepared in 100-nm-diameter pores of PC membrane. (e–g) Low- and high-resolution TEM images of Au nonowires grown electrochemically (e,g) and chemically (f) inside $(TiO_2/PSS)_9TiO_2$ tubules. (b,c,f) Scale bar = 50 nm.

plating the bottom metal electrode [20], layer-by-layer assembly of the multilayer film, electroplating the top metal electrode, and dissolving the template in 1 M NaOH or CH_2Cl_2. Layer-by-layer assembly of (TiO_2 or ZnO)/(PAN or PSS) multilayer film onto the exposed tips of the metal nanowires was achieved by subjecting the metal-filled membrane to the same procedure as that used for planar substrates [30,31]. However, adsorption and washing times were increased to 15–30 min. Control experiments on planar metal substrates showed that no priming procedure was needed for the silver bottom electrode, but that priming of the gold electrode surface with mercaptoethylamine (MEA) (24 h adsorption of MEA from a 5% ethanolic solution) should precede the deposition of multilayer (TiO_2 or ZnO)/polymer films.

2.2. Device structures in which the semiconductor/polymer film covers the walls of a rod-shaped electrode

For preparing these structures, two strategies were applied.

(1) Layer-by-layer synthesis of multilayer TiO_2/PSS or ZnO/PSS tubules on the pore walls followed by electrochemical or chemical plating of Au rods inside the tubules is shown in Fig. 2. Before tubule growing, a PC membrane was soaked in 1% aqueous PEI for 2.5 h. A membrane was successively immersed in aqueous TiO_2 (4 wt.%, pH 2) or ethanolic ZnO (0.17 M) and PSS (1 wt.%) stock solutions for 15 min. After each immersing step, the membrane was placed in a suction filtering unit and washed with two 15-ml portions of 0.01 M aqueous HCl or EtOH and water,

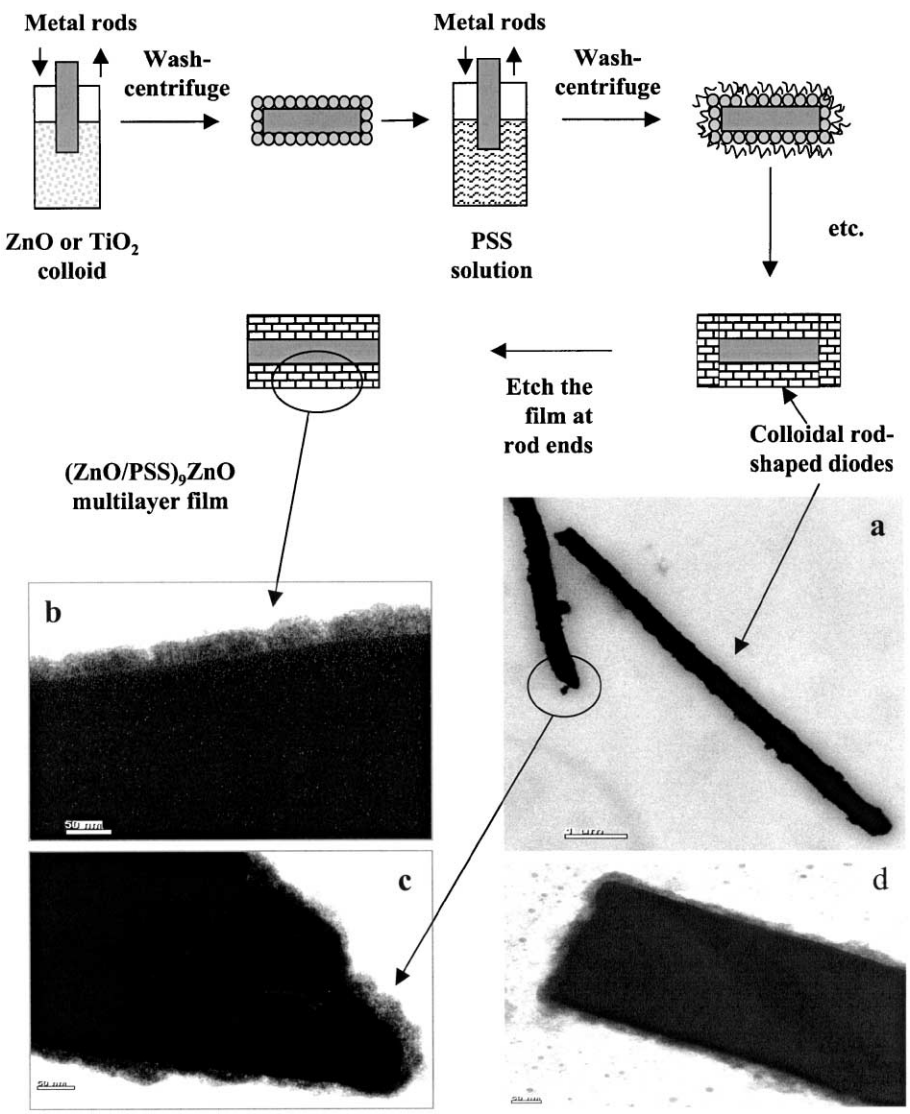

Fig. 3. (Top) Scheme for layer-by-layer assembly of semiconductor/polymer film on the surface of template-grown metal nanowires. (Bottom) (a–d) Low- and high-resolution TEM images of Au nanowires that were grown in alumina membrane, then released with HNO_3 and NaOH and subjected to 10 ZnO/PSS (a–c) or 3 PSS/TiO_2 (d) adsorption cycles. One can see the nanoparticle film completely covering the walls and ends of the rods. (b–d) Scale bar = 50 nm.

respectively, under vacuum followed by drying in Ar stream. Au rods inside the TiO_2/PSS tubules were grown using electrochemical or electroless [15] technique.

(2) Layer-by-layer deposition of ZnO/PSS or TiO_2/PSS films on the surface of metal nanowires was performed as follows. Eight-micrometer-long gold rods were grown electrochemically and transferred into ethanolic solution [20]. Then the gold surface was derivatized with MEA. The layer-by-layer assembly of multilayer ZnO/PSS or PSS/TiO_2 film on the primed surface of the nanowire was conducted as presented in Fig. 3. Ethanolic ZnO or aqueous TiO_2 and aqueous PSS were alternately added to the concentrated (by centrifuging) suspension of nanowires in the appropriate solvent. Each 5-min adsorption cycle was followed by a centrifugation/washing cycle with the appropriate solvent, which was then replaced by the solvent used in the next adsorption step.

Nanowires were aligned for electrical measurements using electrofluidic technique [40].

3. Results and discussion

3.1. Device structures in which the semiconductor/polymer films are sandwiched between two segments of a nanowire (Fig. 1)

TEM images (not shown) of gold nanowires grown in alumina membranes show that the growing ends of the wires are cup shaped. Recently, we have shown that such a cup may be about 100 nm deep, and that TiO_2 nanoparticles adsorb on the bottom and wall of the cup [38]. The tip shape (which can influence the uniformity and continuity of nanoparticle junctions between metal segments) can be altered by passivation of the pore walls of alumina membranes by alkylsilane derivatives, such as chloromethylsilane, triethoxyethylsilane and OTS. Transmission IR spectra of an alumina membrane treated with OTS showed new intense bands characteristic of OTS [38]. TEM images of Au nanowires grown from OTS-treated alumina show a tendency for the otherwise cup-shaped end to become convex and pointed. Thus, the hydrophobization of the pore walls allows to some extent smoothing the surface of the rod ends.

Optical micrographs (not shown) of the suspended Au/$(TiO_2$/PAN$)_9TiO_2$/Pt or Au/Ag/$(TiO_2$/PSS$)_9TiO_2$/Au nanowires clearly show the presence of silver or platinum segments in the nanowires. In a TEM image of Au/Ag/$(ZnO$/PAN$)_9$ ZnO/Au nanowires prepared in 70-nm pores of the PC membrane, one can see the metal/nanoparticle film/metal junction (Fig. 1d). However, a TEM image (recorded within the first several seconds) of Au/$(TiO_2$/PAN$)_{10}$/Ag/Au nanowire, which was prepared in 200-nm pores of the alumina membrane, shows no visible signs of a metal/film/metal junction (Fig. 1c). In the alumina membrane, the metal ions used in the second electrodeposition step fill voids between nanoparticle film and pore walls, so that the top electrode follows the tip surface of the bottom electrode resulting in apparently featureless nanowire walls. This process is promoted by the strong affinity of the metal ions to the alumina pore walls. During TEM imaging, focusing the electron beam on this featureless nanowire for several seconds leads to beam-induced metal melting near the Au/film/Ag junction (Fig. 1b). A break appears in the wire, and particles of 5–10 nm diameter, which adhere to both metal ends, are observed (Fig. 1a). Apparently, the TiO_2 nanoparticles are present between the two electroplated metal segments. Optical and TEM data confirm that a multilayer TiO_2/polymer film can be assembled layer by layer on the tip of a metal rod in the membrane, and that this film does not prevent electroplating the second metal segment on the top of the film.

3.2. Device structures in which a semiconductor / polymer film covers the walls of a nanowire

TEM images of $(TiO_2$/PSS$)_5TiO_2$ tubules grown on the alumina membrane pore walls and released by membrane dissolution are shown in Fig. 2a,b. The tubules are typically 5–15 μm long and their walls are rather dense and uniformly thick. Fig. 2c shows TiO_2/PSS tubules of the same composition but grown inside 200-nm pores of a PC membrane. The latter tubules also have densely packed walls of approximately the same thickness, but unlike those grown in alumina, they are broken and never longer than 1–1.5 μm. A four-layer ZnO/PSS tubule, prepared inside the 100-nm pores of a PC membrane, has ~10-nm thick walls, which is in reasonable agreement with ellipsometric thickness (~3 nm per ZnO/PSS) of planar ZnO/PSS films. The outside surface of all the tubules is quite smooth, and its geometry follows the geometry of the pore walls. These observations suggest strong adsorption of the first TiO_2 and ZnO particle layer on both alumina and PC surfaces. Previously, we showed that TiO_2 colloidal particles readily form a well-packed monoparticle layer on a planar Al/Al_2O_3 substrate [31]. However, breaking of the tubules released from PC membranes is observed always and may be due to the swelling of PC membranes in solutions used to prepare the tubules and dissolve the membrane.

Electrochemical or electroless gold plating inside the multilayer TiO_2/PSS tubules results in solid metal rods with walls bearing a thin nanoparticle film (Fig. 2e–g). The film on the electrochemically grown nanowire looks featureless and smoother than that grown on an electrolessly prepared nanowire (Fig. 2e,f). Its roughness, which is determined by roughness of the pore walls, is comparable with average size of the TiO_2 colloidal particles, ~5 nm. The metal-filled TiO_2/PSS tubules tend to break near their ends thus leaving metal tips accessible for further

derivatization by chemical techniques. The length of the nanowires is in the range of 3–5 μm for electrochemical plating (Fig. 2g) and 2–12 μm for electroless plating.

3.3. Layer-by-layer assembly of film on the surface of template-grown nanowires released from the membrane (Fig. 3)

This method, in contrast to the one described above, is applicable to a wide range of films, which are destroyed under conditions applied to dissolve the template membrane. The Au nanowires subjected to 10 ZnO/PSS adsorption cycles are shown in Fig. 3a–c. One can see that this synthetic technique results in nanowires with covered walls (Fig. 3b) and ends (Fig. 3c). To prepare nanowires with the ends accessible for further functionalization, one should start with a sacrificial metal (e.g. Ag or Cu) at the tips of the wires. The film thickness is approximately 25 nm, which is slightly less than expected, since on planar Au substrates, the average thickness per ZnO/PSS adsorption cycle is 3 nm per ZnO/PSS. This difference tends to increase with the number of adsorption cycles. The thick-

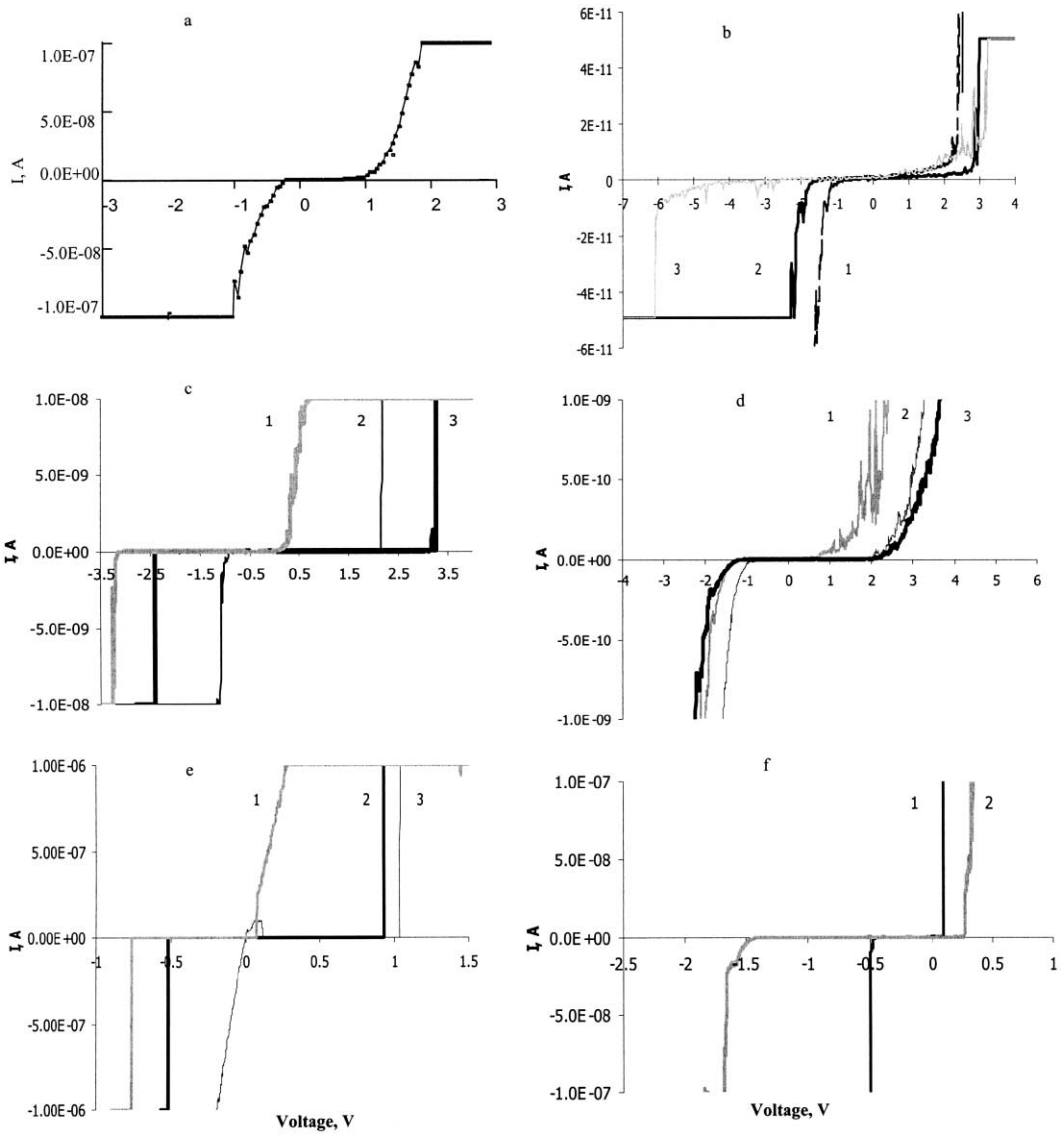

Fig. 4. *I–V* characteristics of nanowire devices measured in air at ambient temperature: (a) in-rod Au(MEA)/$(TiO_2/PAN)_3TiO_2$/Pt device, sweep starts from −7 V; (b) planar Au/TiO_2/Pt (1), Au(MEA)/$(TiO_2/PAN)_9TiO_2$/Pt (2) and Au/PAN/Pt (3) devices, device area ~2 μm^2, all sweeps start from −7 V; (c) concentric Au/$(TiO_2/PSS)_9TiO_2$/Ag device, sweeps 1 and 2 start from 4 and −3 V, respectively, curve 3 was measured in two sweeps starting from 0 V each; (d) concentric Au(NH_2)/$(ZnO/PSS)_{19}ZnO$/Ag device, sweeps 1 and 2 start from 6 and −3 V, respectively, curve 3 was measured in two sweeps starting from 0 V each; (e) planar Au(NH_2)/$(TiO_2/PSS)_9TiO_2$/Ag, device area ~1 μm^2, sweeps 1 and 3 start from 2 and −1 V, respectively, curve 2 was measured in two sweeps starting from 0 V each; (f) planar Au/PSS/Ag (1) and Au/TiO_2/Ag device area ~1 μm^2, sweeps 1 and 2 start from 1 V. In all cases, the nanowires were positioned between lithography-prepared two gold pads by AC electrofluidic alignment [40] and 175-nm-thick gold pads were evaporated on the top of metal ends. Electrical contact with semiconductor/polymer film in concentric devices was made by evaporation of 30-nm-thick Ag stripe on the top of Au rod bearing ZnO/PSS or TiO_2/PSS multilayer film on the walls.

ness of a three-layer PSS/TiO_2 film, ~15 nm (Fig. 3d), somewhat exceeds that expected from ellipsometric data (~4 nm per TiO_2/PSS).

4. Electrical properties

An in-wire Au(MEA)/$(TiO_2/PAN)_3TiO_2$/Pt device (Fig. 4a) shows current rectifying behaviour with turn-on potentials at ~−0.2 and ~+0.9 V for forward and reverse bias, respectively. The difference in turn-on potentials (0.7 V) is higher than that expected from the difference in work functions of Pt (~5.6 eV) and Au (~5.3 eV), while the turn-on potentials are lower than barrier heights at the metal/film interfaces that might be expected from the TiO_2 conduction band edge potential (~4.0 eV). The *I–V* characteristic of a planar Au(MEA)/$(TiO_2/PAN)_9TiO_2$/Pt device shows a difference in turn-on potentials as high as 1.12 V (Fig. 4b-2). Comparing both *I–V* curves to those for bare Au/TiO_2/Pt (Fig. 4b-1) and Au/PAN/Pt (Fig. 4b-3) planar devices suggests that the TiO_2 particles are responsible for the rectifying behavior, because PAN shows insulating behavior in the voltage range of −5 to +3 V. It should be noted that all the *I–V* curves described above were measured in a single positive-going sweep starting from −7 V.

Au/$(TiO_2/PSS)_9TiO_2$/Ag structures prepared as concentric device (Fig. 4c-1,2), in which the TiO_2/PSS film covers the Au-nanowire walls and is in contact with a silver electrode evaporated top, and previously reported in-wire devices of the same composition [38], show similar *I–V* behaviour. When the *I–V* curves are obtained in single sweeps starting from either negative or positive potentials, enhanced asymmetry is seen compared to curves measured in two sweeps starting from 0 V each. The same tendency is found for planar Au(MEA)/$(TiO_2/PSS)_9TiO_2$/Ag devices (Fig. 4e) and bare Au/TiO_2/Ag (Fig. 4f-2) and Au/PSS/Ag (Fig. 4f-1) structures. One possible explanation for this hysteresis is the localization of injected charge carriers at interface and surface states. Saturation and emptying of surface traps is a slow process that can determine the current flow on this time scale. This idea is supported by the observation of current (see, e.g. Fig. 4e-3) immediately after switching the voltage and the subsequent decrease in current by several orders of magnitude. The nature of the traps is not understood at present; they cannot be unambiguously assigned to either TiO_2 particles or PSS chains since both bare Au/TiO_2/Ag (Fig. 4f-2) and Au/PSS/Ag (Fig. 4f-1) structures show similar behavior.

It is interesting to note that the hysteresis for an Au(NH_2)/$(ZnO/PSS)_{19}$ZnO/Ag structure prepared as a concentric device (Fig. 4d), although it exists, is much less pronounced than that of the TiO_2/PSS thin-film devices. One can assume that surface states of the semiconductor particles affect the electrical properties of semiconductor/polymer films. We have shown earlier [38] that rectification in Au(NH_2)/$(ZnO/PSS)_{19}$ZnO/Ag structures is determined by charge injection at the metal/ZnO/PSS–film interface rather than by a tunneling mechanism, while the charge transport in Au/$(TiO_2/PSS)_9TiO_2$/Ag structures cannot be described quantitatively by either Schottky or Fowler–Nordheim equations.

The very different shapes of the *I–V* curves for TiO_2/PSS and TiO_2/PAN thin-film structures suggest that the polymer component also exerts an influence on the rectifying properties of these devices. Currently, the layer-by-layer synthetic technique does not allow one to control the lateral structure of multilayer films. Due to phase boundaries in the organic and inorganic layers (at least in the case of 3D particles), the formation of inhomogeneous contacts, in which both the semiconductor and polymer touch the metal surface, is possible. Without knowing the details of the interfacial composition, it is difficult to arrive at a complete understanding of the electrical properties. Nevertheless, the observed hysteresis holds some promise for use in memory devices.

5. Conclusions

Both concentric and in-wire semiconductor-containing films cause current rectifying effects in “striped” metallic nanowires. Current rectification appears to arise at the interface between the high work function metal (Au or Pt) and the oxide semiconductor nanoparticles. Charge trapping effects that are manifested in the current–voltage curves suggest that semiconductor surface states are important in these devices. The observation of hysteresis in the current–voltage properties of these nanowires is surprising and potentially interesting in terms of switching devices. At present, the reason for this hysteresis is not well understood. There are clear differences in the properties of devices prepared from ZnO and TiO_2 nanoparticles, the latter showing larger hysteresis than the former. Whether this hysteresis is also a consequence of electronic effects, such as filling/emptying of surface trap states, or whether it arises from field-induced reorganization of the thin film structure, is currently unknown. Future work will attempt to address the mechanism of these effects in polyelectrolyte/oxide semiconductor devices.

Acknowledgements

We thank the DARPA Moletronics Program and the Office of Naval Research for support of this work.

References

[1] H. Abruña, P. Denisevich, M. Umana, T.J. Meyer, R.W. Murray, J. Am. Chem. Soc. 103 (1981) 1.
[2] P. Denisevich, K.W. Willman, R.W. Murray, J. Am. Chem. Soc. 103 (1981) 4727.

[3] P.G. Pickup, W. Kutner, C.R. Leidner, R.W. Murray, J. Am. Chem. Soc. 106 (1984) 1991.
[4] G.P. Kittlesen, H.S. White, M.S. Wrighton, J. Am. Chem. Soc. 107 (1985) 7373.
[5] G.P. Kittlesen, M.S. Wrighton, J. Mol. Electron. 2 (1986) 23.
[6] L.S. Roman, M. Berggren, O. Inganas, Appl. Phys. Lett. 75 (1999) 3557.
[7] J. Chen, M.A. Reed, A.M. Rawlett, J.M. Tour, Science 286 (1999) 1550.
[8] R.M. Metzger, B. Chen, U. Höpfner, M.V. Lakshmikantham, D. Vuillaume, T. Kawai, X. Wu, H. Thachibana, T.V. Hughes, H. Sakurai, J.W. Baldwin, C. Hosch, M.P. Cava, L. Brehmer, G.J. Ashwell, J. Am. Chem. Soc. 119 (1997) 10455.
[9] J.C. Ellenbogen, J.C. Love, Proc. IEEE 88 (2000) 386.
[10] T. Rueckes, K. Kim, E. Joselevich, G.Y. Tseng, C.-L. Cheung, C.M. Lieber, Science 289 (2000) 94.
[11] C.P. Collier, E.W. Wong, M. Belohradsky, F.M. Raymo, J.F. Stoddart, P.J. Kuekes, R.S. Williams, J.R. Heath, Science 285 (1999) 391.
[12] C.P. Collier, G. Mattersteig, E.W. Wong, Y. Luo, K. Beverly, J. Sampaio, F. Raymo, J.F. Stoddart, J.R. Heath, Science 289 (2000) 1172.
[13] D. Al-Mawlawi, C.Z. Liu, M. Moskovits, J. Mater. Res. 9 (1994) 1014.
[14] M. Nishizava, V.P. Menon, C.R. Martin, Science 268 (1995) 700.
[15] V. Menon, C.R. Martin, Anal. Chem. 67 (1995) 1920.
[16] C.R. Martin, Chem. Mater. 8 (1996) 1739.
[17] L. Wang, K. Yu-Zhang, A. Metrot, P. Bonhomme, M. Troyon, Thin Solid Films 288 (1996) 86.
[18] C.R. Martin, R.V. Parthasarathy, Adv. Mater. 7 (1995) 487.
[19] B.B. Lakshmi, P.K. Dorhout, C.R. Martin, Chem. Mater. 9 (1997) 857.
[20] B.R. Martin, D.J. Dermody, B.D. Reiss, M. Fang, L.A. Lyon, M.J. Natan, T.E. Mallouk, Adv. Mater. 11 (1999) 1021.
[21] J.K.N. Mbindyo, B.D. Reiss, B.R. Martin, C.D. Keating, M.J. Natan, T.E. Mallouk, Adv. Mater., in press.
[22] B.D. Reiss, J.N.K. Mbindyo, B.R. Martin, S.R. Nicewarner, T.E. Mallouk, M.J. Natan, C.D. Keating, Mater. Res. Soc. Symp. Proc., in press.
[23] J.H. Fendler, F. Meldrum, Adv. Mater. 7 (1995) 607.
[24] T.E. Mallouk, H.-N. Kim, P.J. Ollivier, S.W. Keller, in: G. Alberti, T. Bein (Eds.), Comprehensive Supramolecular Chemistry, vol. 7, Elsevier, Oxford, UK, 1996, p. 189.
[25] G. Decher, Science 277 (1997) 1232.
[26] S.W. Keller, H.-N. Kim, T.E. Mallouk, J. Am. Chem. Soc. 116 (1994) 8817.
[27] V.L. Colvin, A.N. Golstein, A.P. Alivisatos, J. Am. Chem. Soc. 114 (1992) 5221.
[28] E.R. Kleinfeld, G.S. Ferguson, Science 265 (1994) 370.
[29] J.H. Fendler, Chem. Mater. 8 (1996) 1616.
[30] N. Kovtyukhova, P.J. Ollivier, S. Chizhik, A. Dubravin, E. Buzaneva, A. Gorchinskiy, A. Marchenko, N. Smirnova, Thin Solid Films 337 (1999) 166.
[31] N. Kovtyukhova, A. Gorchinskiy, C.C. Waraksa, Mater. Sci. Eng. B69–70 (2000) 424.
[32] T. Cassagneau, J.H. Fendler, T.E. Mallouk, Langmuir 16 (2000) 241.
[33] T. Cassagneau, T.E. Mallouk, J.H. Fendler, J. Am. Chem. Soc. 120 (1998) 7848.
[34] D.L. Feldheim, K.C. Grabar, M.J. Natan, T.E. Mallouk, J. Am. Chem. Soc. 118 (1996) 7640.
[35] M. Gao, B. Richter, S. Kirstein, H. Mohwald, J. Phys. Chem. 102 (1998) 4096.
[36] D.M. Kaschak, J.T. Lean, C.C. Waraksa, G. Saupe, H. Usami, T.E. Mallouk, J. Am. Chem. Soc. 121 (1999) 3435.
[37] J.S. Yu, J.Y. Kim, S. Lee, J.K.N. Mbindyo, B.R. Martin, T.E. Mallouk, J. Chem. Soc., Chem. Commun. (2000) 2445.
[38] N.I. Kovtyukhova, B.R. Martin, J.K.N. Mbindyo, P. Smith, B. Razavi, T.S. Mayer, T.E. Mallouk, J. Phys. Chem., submitted for publication.
[39] J.C. Chiang, A.G. MacDiarmid, Synth. Met. 13 (1986) 193.
[40] P.A. Smith, C.D. Nordquist, T.N. Jackson, T.S. Mayer, B.R. Martin, J. Mbindyo, T.E. Mallouk, Appl. Phys. Lett. 77 (2000) 1399.